

THE EFFECT OF AGING TREATMENT ON MECHANICAL PROPERTIES OF AA6082 ALLOY: MODELING AND EXPERIMENT

N. Anjabin and A. Karimi Taheri*

* ktaheri@sharif.edu

Received: January 2010

Accepted: April 2010

Department of Materials Science and Engineering, Sharif University of Technology, Tehran, Iran.

Abstract: A novel constitutive equation has been proposed to predict the effect of aging treatment on mechanical properties of AA6082 aluminum alloy. Considering that aging phenomenon affects the distribution of alloying element in matrix, and the fact that different distribution of alloying elements has different impediments to dislocation movement, a material model based on microstructure, has been developed in this research. A relative volume fraction or mean radius of precipitations is introduced into the flow stress by using the appropriate relationships. The GA-based optimization technique is used to evaluate the material constants within the equations from the uni-axial tensile test data of AA6082 alloy. Finally, using the proposed model with optimized constants, the flow behavior of the alloy at different conditions of heat treatment is predicted. The results predicted by the model showed a good agreement with experimental data, indicating the capability of the model in prediction of the material flow behavior after different heat treatment cycles. Also, the calculated flow stress was used for determination of the material property in Abaqus Software to analyze the uniaxial compression test. The force- displacement curves of the analysis were compared to the experimental data obtained in the same condition, and a good agreement was found between the two sets of results.

Keywords: Aluminium alloys, Heat treatments, Mechanical properties, FEM analyze.

1. INTRODUCTION

Aluminium alloys have a wide usage in industrial application because of their high strength to weight ratio. In this regard, the age hardenable alloy due to their higher strength achieving from aging process, have more applicability [1,2]. These alloys in aged condition have a high flow stress and relatively low ductility, which refers to impediment of precipitates to movement of mobile dislocations. Moreover, the probability of crack initiation at second phase/matrix interface may reduce ductility [3]. The flow behavior of these alloys, has received a large number of studies, and several theoretical model have been proposed to analyze the flow behavior [3-10]. In majority of the mentioned models, the hardening process has been considered as a competition between dislocation pile up and dislocation annihilation phenomena during forming [4-8]. It has been reported that the chemical composition, production technology, and heat treatment, all affect the precipitation process as well as the amount of strengthening [11]. Although these models are based on microstructure evolution during forming and have a relatively good agreement with experimental results, they have

not considered the effects of distribution of chemical elements in matrix, which in turn noticeably is affected by preceding heat treatment. In this research, in order to develop a model, based on microstructure evolution during deformation and capable to capture the influence of aging treatment parameters, in both underage and overage conditions, the semi experimental relationships relating the precipitations size or volume fraction to the flow stress, is coupled with a dislocation evolution model. The constants in extended constitutive equations thereby derived, are determined using an optimization technique with the aid of genetic algorithm and experimental data of AA6082 alloy. To verify the results predicted by the model, the uniaxial compression was analyzed using the Abaqus software and the results were compared with the experimental results.

2. MATHEMATICAL MODELING

Dislocation glide is the major mechanism for the plastic deformation of most alloys including aluminum alloys [11]. For this reason flow stress can be evaluated by considering the barriers to the motion of dislocations. These barriers can be divided into impediments of dislocations and

friction stresses. Hence the following assumption for the flow stress is reasonable [4,10]:

$$\sigma = \sigma_f + \sigma_w \quad (1)$$

where σ_f is the friction stress and σ_w , is due to the interaction of the dislocations with each other.

3. THE STRENGTH OF DISLOCATION IMPEDIMENTS

The contribution of dislocation density on flow stress can be obtained as follows [4,6,9];

$$\sigma_w = \alpha G b \sqrt{\rho} \quad (2)$$

where ρ , is the total dislocation density, G the shear modulus, b the magnitude of the Burger's vector, and α a constant of order of unity.

To determine the variation of the total dislocation density of deforming metal, the proposed equation by kocks-Mecking [4-8], can be employed as follows:

$$\frac{d\rho}{d\varepsilon^p} = k_1 \sqrt{\rho} - k_2 \rho \quad (3)$$

where k_1 represents the rate of dislocation storage and is considered as a constant, and k_2 represents the rate of dislocation recovery occurring by dislocation cross slip at low temperatures. Thus, k_2 is affected by heat treatment.

Integration of Eq. (1) and Eq. (2) and using the boundary condition of $\varepsilon^p = 0$ at $\rho = \rho_0$, leads to the following equation:

$$\sigma_w = \alpha G b \left[\sqrt{\rho_0} + \left(\frac{k_1}{k_2} - \sqrt{\rho_0} \right) (1 - \exp(\frac{-1}{2} k_2 \varepsilon^p)) \right] \quad (4)$$

4. FRICTION STRESS

This part of flow stress is due to the impediments of solute atoms, precipitations, dispersion, grain and twin boundaries, and so on, to dislocation movements. Often the following assumption is acceptable for the friction stress [13-15]:

$$\sigma_f = \sigma_{ss} + \sigma_{ppt} + \sigma_i \quad (5)$$

where, σ_{ss} is the solution hardening component, σ_p the precipitation hardening component, and σ_i the intrinsic strength of the pure aluminum, that can be assumed as a constant.

Referring to this equation one should consider how the alloying elements are distributed in the matrix to affect the friction stress. As the alloying elements distributions are mainly affected by aging heat treatments, the friction stress can be evaluated with aging progress as follows:

5. AGING TREATMENT

Aging treatment alters the microstructure of metal, from 1) solid solution with incompatible atoms to 2) distribution of fine coherent precipitation surrounded by elastic strains to 3) coarse and distributed particles with incoherent interfaces [1,11]. These structures have different strength to the motion of dislocations.

Since the strengthening mechanisms in aging process are different at the early and final stages [11,13], the discussion can be performed in terms of underage and overage condition, separately.

6. UNDERAGE CONDITION

6.1. Precipitation Hardening

Although the interacting force between the moving dislocation and precipitates mainly depends on the strengthening mechanism [13,14], the theoretical analyzes have shown that the barrier strength and the volume fraction are proportionate, for almost all of the strengthening mechanisms and when the precipitates are shearable [13]. On the other hand, investigations have shown that the contribution from precipitates to flow stress depends on the critical dislocation breaking angle.

Obstacles are considered 'strong' if the breaking angle is smaller than 120° or 'weak' when the breaking angle is larger than 120° [14].

The contribution from weak and strong obstacle to flow stress can be obtained as follows [12-14]:

$$\sigma_{ppt} \Big|_{strong} = C_1 (f_r^{\frac{1}{2}}) \quad (6)$$

$$\sigma_{ppt} \Big|_{weak} = C_2 (rf_r^{\frac{1}{2}}) \quad (7)$$

where C_1 and C_2 are constants, r is the mean precipitates radius, and f_r the relative volume fraction of precipitates, defined as:

$$f_r = \frac{f}{f_{peak}} \quad (8)$$

where f and f_{peak} are precipitate volume fraction in underage and peak age condition, respectively.

Assuming a spherical shape for any particle one can write;

$$r = r_{peak} (f_r^{\frac{1}{3}}) \quad (9)$$

Considering Eq. (6), Eq. (7), and Eq. (9) for precipitation strengthening, one can write:

$$\sigma_{ppt} = b_1 (f_r^{m_1}) \quad (10)$$

where m_1 can take an amount between $\frac{1}{3}$ to $\frac{2}{3}$, when there is a mixture of weak and strong particles, and b_1 is the amount of stress in peak age condition, depending strongly on aging temperature [1,11]. This dependency can be obtained by introducing an Arrhenius type equation as follows:

$$b_1 = b_{01} \exp\left(-\frac{Q_1}{RT}\right) \quad (11)$$

where b_{01} and Q_1 are constants.

5. SOLID SOLUTION HARDENING

The contribution of solid solution strengthening, σ_{ss} , to friction stress is related to relative volume fraction of precipitates, f_r , in the matrix [12,13,14];

$$\sigma_{ss} = \sigma_{0ss} (1 - \alpha f_r)^{\frac{2}{3}} \quad (12)$$

where σ_{0ss} is the solid solution contribution in as-quenched condition. So, for a given alloy we

can assume σ_{0ss} as a constant. α is the fraction of the as-quenched solute concentration (assuming a quasi-binary system) depleting from the matrix when f_r approaches unity at the peak-age condition.

6. KINETIC OF AGING

Referring to Eq. (10) and Eq. (12), it is observed that the strength calculation needs knowledge of evolution of relative volume fraction of precipitates during aging. Prior investigations have shown that, JAMAC kinetic equation can be used to evaluate the aging kinetics, because aging phenomenon is a nucleation and growth phenomena [13,16].

$$f_r = 1 - \exp(-kt^n) \quad (13)$$

where k and n are JMAC parameters. n is considered as a constant. But k depends on temperature as follows:

$$k = k_0 \exp\left(-\frac{Q_k}{RT}\right) \quad (14)$$

where k_0 and Q_k are constants.

7. OVERAGE CONDITION

Investigations have shown that, after peak age conditions, due to decrease in coherency strains around precipitates and increase in precipitates distance with increasing aging time, the flow stress decreases [11].

In overaging condition, the volume fraction of precipitations remains constant and only the particle coarsening is occurred. Hence, the solid solution hardening component can be determined using Eq. (12) with $f_r=1$. In over age condition, the precipitation hardening is related to precipitation size as follows [13,14]:

$$\sigma_{ppt} = b_2 (r^{m_2-1}) \quad (15)$$

where b_2 is the amount of stress in peak age condition where it is strongly depended on aging temperature. At this condition, an Arrhenius type equation is introduced:

$$b_2 = b_{02} \exp\left(-\frac{Q_2}{RT}\right) \quad (16)$$

where b_{02} and Q_2 are constants.

8. KINETICS OF PARTICLE COARSENING

To estimate the evolution of r during overageing, a coarsening law can be utilized as follows [13]:

$$r^3 - r_{peak}^3 = k_c (t - t_{peak}) \quad (17)$$

where the rate constant k is given by:

$$k_c = \frac{B}{T} \exp\left(-\frac{Q_B}{RT}\right) \quad (18)$$

where B and Q_B are constants.

and t_{peak} is the time required to reach the peak age condition. t_{peak} depends on aging temperature in such a way that increasing the aging temperature results in decrease in peak time. So, the following relationship proposed by Eivani and Karimi Taheri [16], can be used.

$$t_{peak} = \left(\frac{t_0}{T}\right)^{n_1} \quad (19)$$

where t_0 and n_1 are constants.

Using the above set of equations, one can estimate the flow stress at room temperature in the plastic region, after different aging treatment cycles.

9. DETERMINATION OF THE MATERIAL CONSTANTS FOR THE CONSTITUTIVE EQUATION

Some of the parameters in the present model can be selected beforehand (Table 1). The rest is

Table 1. Material constants selected in this research

| | |
|--------------------------------|---------------|
| $\alpha = 1$ | From Ref. [7] |
| $G_{ref} (MPa) = 26354$ | From Ref. [7] |
| $b(m) = 2.857 \times 10^{-10}$ | From Ref. [7] |

determined by the optimization techniques based on minimizing the sum of the square of the errors between the experimental and computed data. An objective function for these particular problems [17,18] is :

$$f(x) = \sum_{j=1}^M \sum_{i=1}^{N_j} \{W_{ij} \left[\frac{\sigma_{ij}^e - \sigma_{ij}^c}{\sigma_{N_{jj}}^e} \right]^2\} \quad (20)$$

where $W_{ij} = \frac{\sigma_{ij}^e}{\sum_{j=1}^M \sum_{i=1}^{N_j} (\sigma_{ij}^e)}$ is the weighting function for stress.

M corresponds to the number of the experimental curves, and N_j to the number of data points for the j th computed curve. $\sigma_{N_{jj}}^e$ refers to the maximum magnitudes of the experimental stress for j th experimental curve. σ_{ij}^c and σ_{ij}^e are computational and experimental stress for the same strain level and correspond to the i th computed and experimental data points for j th computed and experimental curve, respectively. x represents the constants vector. The calculated stress σ_{ij}^c has to be determined from the constitutive equations.

The objective function $f(x)$ requires the global minimization subjected to determining the optimum value of each constant. The traditional graphical approach to determine material constants using experimental data often requires decreasing the problem to a linear equation between two variables, while the rest assumed to be constants. Using this approach needs performing a large number of experimental tests. Therefore, there is an increasing trend in using numerical optimization, especially when the number of constants is large, as in this practice. One of the most difficult task in determining the material constants is how to choose the initial values of the constants. In more of these techniques, if the initial values are not properly selected, optimum values cannot be obtained. Using Genetic Algorithms techniques has overcome this problem, because in this algorithm the initial values are selected randomly [17].

In this research the material constants were determined from the experimental data of AA6082 alloy by the following procedure:

The received material was in the form of rod.

Table 2. Aging heat treatment procedure

| Aging temperature | Aging time | | | |
|-------------------|------------|-----|-----|-----|
| | 8 h | 16h | 31h | 48h |
| 160 °C | 8 h | 16h | 31h | 48h |
| 180 °C | 1.5 h | 3h | 32h | --- |
| 200 °C | 30 min | 2h | 6h | 14h |



Fig. 1. True stress vs true plastic strain for underage condition at aging temperature a)160°C, b)180°C, c)200°C, (symbols represents experimental curves and solid lines shows the curves obtained model).

The tensile specimens were machined from the

rod and subjected to aging treatment according to Table 2, after solution treating at 525°C and water quenching. Subsequently, the uniaxial tensile test was carried out at room temperature.

The experimental curves (symbols) for both underage and overage conditions presented in Figs. (1) and (2), have been plotted until the maximum flow stress. As it is seen from Figs. (1)

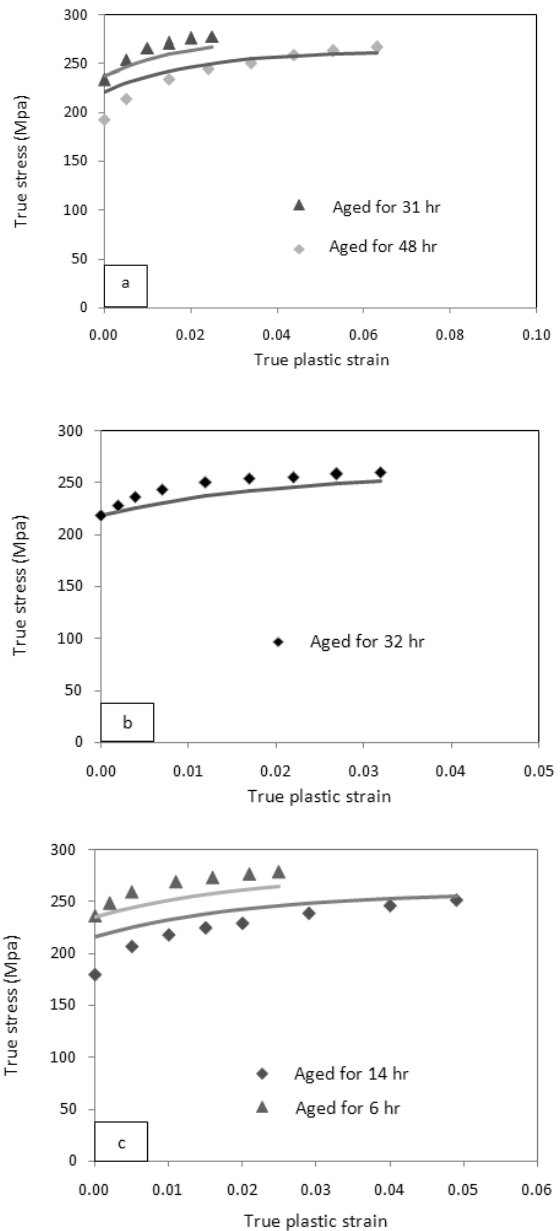


Fig. 2. True stress vs true plastic strain for overage condition at aging temperature a)160°C, b)180°C, c)200°C, (symbols represents experimental curves and solid lines shows the curves obtained model).

Table 3. Material constants determined by the GA optimization technique

| | | |
|--|-------------------------|-------------------------------------|
| $k_1 (m^{-1}) = 7.9 \times 10^8$ | $b_{04} (MPa) = 154.9$ | $Q_k (J/mol) = 5.7 \times 10^4$ |
| $k_2 (underage) = 72.05$ | $Q_4 (J/mol) = 203.5$ | $n = 0.62$ |
| $k_2 (overage) = 97.67$ | $m_1 = 0.66$ | $n_1 = 682.4$ |
| $\rho_0 (m^{-2}) = 6.4 \times 10^{12}$ | $b_{05} (MPa) = 0.39$ | $t_0 = 24.63$ |
| $\sigma_i (MPa) = 13.7$ | $Q_5 (J/mol) = 462.6$ | $r_{peak} (m) = 7.9 \times 10^{-9}$ |
| $\sigma_{0ss} (MPa) = 50.1$ | $m_2 = 0.72$ | $B = 3.14 \times 10^{-26}$ |
| $\alpha_2 = 0.83$ | $k_0 = 1.5 \times 10^4$ | $Q_B (J/mol) = 4.3 \times 10^3$ |

a-c, with increasing the aging temperature or aging time in underage condition, the flow stress increases and the uniform elongation decreases.

This event can be explained considering the microstructural changes. By increase in aging time or temperature during underaging, the precipitate/matrix interface transfers from coherent interface to semi coherent one, resulting in a relatively large coherency strain around precipitates. This makes the movement of dislocations through heavily distorted matrix more difficult, so the strength and hardness are increased and consequently ductility is decreased.

In contrast, as shown in Figs. (2) a-c, in the overaging condition, increase in aging time and temperature leads to decrease in flow stress and increase in uniform elongation. In this stage of aging, the thermodynamically stable precipitates are formed. But these stable particles have complicated crystal structure, and they are formed just with incoherent interface. In this stage the particle often are coarse and their distance are so large that dislocations can readily bow between them. Consequently, the strength and hardness are decreased. As aging progresses, the distance between precipitates is more increased, dislocations bowing are become easier and the hardness is more decreased.

The solid curves in the Figs. (1) and (2), are the corresponding best fitted curve through the computations based on constitutive equation with optimized constants using the GA -based optimization technique. The optimized values for material constants for both underage and overage condition are listed in Table 3.

10. VERIFICATION OF THE DEVELOPED CONSTITUTIVE EQUATIONS

To consider the validity of the model predictions, the uniaxial compression test was analyzed with a trade FEM package, Abaqus software. To do so, the flow behavior of material predicted from the presented model was used to determine the material properties by the software. To perform the analysis, the friction coefficient was selected to be 0.6 from Ref. [13] and 70 GPa for young modulus. Fig. (3) a, b, depict the experimental compressive force-displacement curves (symbols) for the specimen aged at 220°C, for two aging times of 40 minute (underage condition) and 4 hour (overage condition). The solid curves in these figures show the software results achieved with the same condition as experimental curves. As it is seen, there is a fairly good agreement between the experimental and software results.

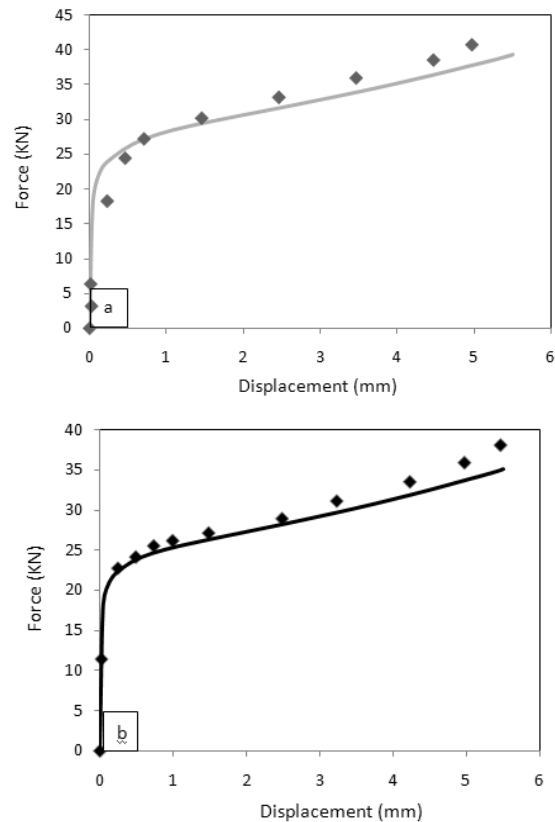


Fig. 3. Force vs displacement for specimen aged at 220 °C for underage (a) and overage (b) conditions, (symbols represents experimental curves and solid lines shows the curves obtained from FEM analyze).



Fig. 4. Variation of relative volume fraction of precipitates during underaging at different temperatures , a) 160 °C, b) 180 °C, c) 200 °C, d) 220 °C.

The variation of relative volume fraction of precipitates during underage condition are predicted and exhibited in Fig. 4. The results indicate that the proposed deformation constitutive equation gives an accurate and almost precise estimate of the flow stress for AA 6082, and can be used to analyze the problems during metal forming process. The minimal deviation may be attributed to the experimental uncertainty.

CONCLUSIONS

1. At a constant aging time, with increasing in aging temperature in underaging condition, the flow stress increases and the uniform elongation decreases. In contrast, in overaging condition the flow stress decreases and the uniform elongation increases. Also, at a constant aging time the same variations as those for the constant aging temperature, are obtained.
2. A material model based on microstructure has been developed in this research. This model is able to predict the flow behavior at room temperature, including the effects of aging treatments variables (i.e. aging time and temperature).
3. An optimization technique based on Genetic algorithm is used to determine the material constants. Such a technique can be used to determine the wide variety of constants in constitutive equations, where the objective function is a nonlinear

function. Also in this approach the difficulty of choosing the best initial values for constants is completely overcome.

4. Using the proposed method to determine the material constants, one only needs to perform a number of simple uniaxial tensile tests, while using traditional method needs a large number of different test, which is time consuming. Hence, the proposed method can be used successfully to simulate the metal forming processes.
5. The material constants of AA6082 alloy were typically determined.
6. Using the proposed model, one can use the material properties in FEM packages such as Abaqus software to analyze a metal forming process.

ACKNOWLEDGMENT

The authors would like to thank Sharif University of Technology for the financial support and the provision of the research facilities used in this work.

REFERENCES

1. Smith, W. F., Structure and Properties of Engineering Alloy, McGraw-Hill Publishing Company, 1981, pp. 162-183.
2. Brooks, C.R., Heat Treatment, Structure and Properties of Nonferrous Alloys, ASM, 1984.
3. Garrett, RP., Lin, J., Dean, TA., An Investigation of the Effects of Solution Heat Treatment on Mechanical Properties for AA 6xxx Alloys: Experimentation and Modelling, Int. J. Plast. 21, 2005, 1640-1657.
4. Bergstrom, Y., A Dislocation Model for the Stress-Strain Behavior of Polycrystalline -Fe with Special Emphasis on the Variation of the Densities of Mobile and Immobile Dislocations, Mater. Sci. Eng., 1969, 193-200.
5. Bergstrom, Y., Hallen, H., An Improved Dislocation Model for the Stress- Strain Behavior of Polycrystalline -Fe", Mater. Sci. Eng. 55, 1982, 49-61.
6. Mecking, H., Kocks, UF., Kinetics of Flow and Strain Hardening, Acta Metall.29, 1981, 1865-1875.

7. Barlata, F., Glazova, MV., Brema, JC., Legea, DJ., A Simple Model for Dislocation Behavior, Strain and Strain Rate Hardening Evolution in Deforming Aluminum Alloys, *Int. J. Plast.* 18, 2002, 919-939.
8. Estrin, Y., Mecking, H., A Unified Phenomenological Description of Work Hardening and Creep Based on One Parameter Models, *Acta. Metall.* 32, 1984, 57-70.
9. Boogaard, V.D., Huetink, J., Simulation of Aluminium Sheet Forming at Elevated Temperatures, *Comput. Methods Appl. Mech. Engrg.* 195, 2006, 6691-6709.
10. Domkin, K., Constitutive Models Based on Dislocation Density, Ph.D. thesis, Lulea University of Technology, 2005.
11. Porter, D. A., Easterlina, A., Phase Transformation in Metals and Alloys 2nd edit, 1933, pp. 373-385.
12. Myhr, OR., Grong, Q., Anderson, SJ., Modeling of the Age Hardening Behavior of Al-Mg-Si alloys, *Acta. Mater.* 49, 2001, 65-75.
13. Esmaeili, S., Lloyd, DJ., Poole, WJ., A Yield Strength Model for the Al-Mg-Si-Cu Alloy AA6111, *Acta Mater.* 51, 2003, 2243-2257.
14. Esmaeili, S., Lloyd, DJ., Poole, WJ., Modeling of Precipitation Hardening for the Naturally Aged Al-Mg-Si-Cu Alloy AA6111, *Acta Mater.* 51, 2003, 3467-3481.
15. Bjqrneklett, BI., Grong, Q., Myhr, OR., Kluken, AO., A Process Model for the Heat – Affected Zone Microstructure Evolution in Al-Zn-Mg Weldments, *Metall. Mater. Trans. A* 30, 1999, 2667-2677.
16. Eivani, A. R., Karimi Taheri, A., Modeling Age Hardening Kinetics of an Al-Mg-Si-Cu Aluminum Alloy, *J. Mater. Process. Tech.* 205, 2008, 388–393.
17. Lin, J., Yang, J., GA Based Multiple Objective Optimization for Determining Visco- Plastic Constitutive Equations for Super Plastic Alloys, *Int. J. Plast.* 15, 1999, 1181-1196.
18. Lin, J., Liu, Y., A Set of Unified Constitutive Equations for Modeling Microstructure Evaluation in Hot Deformation, *J. Mater. Process. Tech.* 143-144, 2003, 281-285.